Particle Velocimetry of Newtonian and non-Newtonian Droplets Impacting a Hydrophobic Surface

M.I. Smith · V. Bertola

Received: date / Accepted: date

Abstract A particle velocimetry technique is described which enables the measurement of the fluid velocity inside impacting drops. Using high speed photography of 2 μm fluorescent tracer particles suspended in the fluid, the velocity field was measured as a function of time and radial position. The potential of the technique is illustrated using velocimetry measurements of drops of pure water and aqueous solutions of 200ppm poly-(ethylene oxide) (PEO). Dilute solutions of PEO have been known for some time to suppress the rebound of water from hydrophobic surfaces. The dissipation has traditionally been attributed to an increased extensional viscosity as the polymers stretch in the extensional flow of the droplet. Our results enable us to infer that the extensional viscosity of PEO drops, during both the spreading and retraction phase, is similar to that of pure water. The data suggests that the true source of dissipation lies at the droplet edge. We also show, by analysing the spreading of water drops, that the Roisman-Yarin theory for a droplet spreading on a surface is valid in the bulk of the droplet prior to the final stages of spreading.

PACS and mathematical subject classification numbers as needed.

Keywords drop impact · PIV · particle image velocimetry · dilute polymer solutions · PEO · hydrophobic · surface · non-Newtonian · extensional viscosity

PACS 47.57.Ng · 47.80.-v · 47.55.D- · 47.50.Ef

Funding by the Engineering and Physical Sciences Research Council, United Kingdom (EP/E005950/1) is also gratefully acknowledged.

M.I. Smith
SMART Laboratory, University of Edinburgh, King's Buildings, Mayfield Rd, Edinburgh, UK
Present address: of M.I. Smith
Dept Physics and Astronomy, University of Nottingham, University Park, Nottingham, UK
E-mail: mike.i.smith@nottingham.ac.uk

V. Bertola
SMART Laboratory, University of Edinburgh, King's Buildings, Mayfield Rd, Edinburgh, UK
tel: +44 (0)131 650 8697 fax: +44 (0)131 650 6551 E-mail: v.bertola@ed.ac.uk

1 Introduction

Particle Image Velocimetry (PIV) has been a recognised technique for 25 years [1–3] and in that time has become an indispensable tool for visualising and quantifying fluid flows. Initial research in the field used laser speckle patterns, generated by particles suspended in the fluid. The phase difference between randomly distributed particles creates an interference or speckle pattern. As the position of particles move with the fluid the speckle pattern shifts with them allowing the fluid motion to be measured. This technique has been developed and applied to a large variety of laminar and turbulent flows including multiphase flows [4].[1]

An alternative method of measuring fluid velocity, and the one which is followed here, is to resolve and track the positions of indiviual particles, which is known as Particle Tracking Velocimetry (PTV). Provided the particles faithfully follow the flow the velocity of the particles can be understood to be the same as that of the suspending fluid (a condition that is satisifed for small particles of similar density to the fluid at relatively low fluid velocities [5]). The particles therefore move along the fluid pathlines enabling the motion to be observed and quantified. In comparison with PIV, PTV allows one to achieve much higher spatial resolution without increasing significantly the particle concentration, which would be necessary to obtain PIV speckle patterns.

Droplet impact on a solid substrate represents an intriguing class of fluid flows. Commercial and academic interest in the field has driven a sizeable research effort, focussed on understanding and controlling droplet deposition [6,7]. Applications are as diverse as inkjet printing, spray cooling, soldering of microelectronics, forensic science and the agrochemical industry [6,8,9]. Despite the apparent importance of understanding drop impact, measurement techniques have to date been largely focussed on macroscopic observables such as the velocity of the contact line or the drop shape (e.g [10,11]). Drop impact has therefore been unable to benefit from the same insights provided by particle imaging in other areas of fluid dynamics. Whilst the literature reports various theoretical [12–14] and the relative numerical solutions [15–17], there is little experimental data to enable these models to be adequately validated in the drop interior.

Drop impact presents certain specific difficulties that make measurement of the fluid flow inside the droplet a challenging problem. Firstly, since a droplet is a few millimetres in diameter, the tracer particles used to track fluid flow must be small ($\sim \mu$m). This requires observations to be made at high magnification. The shape of a small droplet with surfaces of changing curvature adds to the difficulty of making accurate measurements due to refraction and reflection [4]. Ray tracing methods have been developed and used to some success to overcome these limitations for sessile droplets [18] and an early attempt at PIV measurements was carried out in acoustically levitated droplets [19]. Yet such methods would be extremely difficult to implement during the significant deformations associated with drop impact. Secondly, there is the issue of time scale: droplet impact is a fast process with complete spreading of the droplet occurring in just a few milliseconds. With a fluid velocity of 1000mm/s followed at a magnification of 40x with a typical field of view of $\sim$ 0.5mm a 2 micron particle crosses the entire field of view in just 0.5ms. However, to record the discrete position of a particle using a megapixel camera one needs exposure times of order one thousand

[1] For a detailed description of this and other methods of particle image velocimetry see the excellent review by Adrian [5].

times shorter than this. At such short exposure times achieving sufficient illumination is also an important consideration.

During drop impact onto smooth and chemically homogeneous surfaces, and for low or moderate impact kinetic energy, the dynamics are controlled by three key factors: inertia, viscous dissipation and interfacial energy [11]. During the initial stages of impact with the surface the vertical inertia of the falling drop is converted into the horizontal motion of the fluid. Surface tension can also be important depending on the relative magnitude of both terms. This balance is characterised by the dimensionless Weber number ($\rho V_i^2 D_0/\sigma$). As the fluid spreads across the surface the kinetic energy of the fluid is partly dissipated by viscous forces in the fluid. The extent to which viscous dissipation is important in governing drop dynamics is described using the Reynolds number ($\rho V_i D_0/\eta$) which is sometimes used in combination with the Weber number to yield the Ohnesorge number ($We^{0.5}/Re$). Finally, as the drop reaches maximum spreading, surface tension slows expansion storing the remaining kinetic energy of the fluid in the interfacial energy generated through drop deformation. At this point a drop will have the shape of a disk (eventually surrounded by a circular rim), commonly known as a "lamella". Provided the splashing threshold is not exceeded, which is true in the case of our experiments, the disk then begins to retract as the stored interfacial energy is released. If the effects of surface roughness can be neglected this retraction is governed by a balance between interfacial energy and the viscous dissipation, Capillarity ($V_{retraction}\eta/\sigma$) [11]. Importantly, in the context of the present study, this means that if two drops with similar size, density, velocity and surface tension impact a surface, one expects the difference in fluid velocity during spreading is related to the kinematic viscosity. Similarly if two drops with the same interfacial energy spread to form disks of the same diameter on identical surfaces (ie with the same chemical structure and the same surface roughness), differences in the initial retraction velocity, all other factors being equal, are determined by the fluid viscosity.

If the fluid retracts with sufficient velocity it rises in the middle forming a Worthington jet which may subsequently result in the complete rebound of the drop from the surface. It has been known for many years that the addition of a small quantity of a flexible polymer to the fluid completely suppresses rebound [10]. This is due to the reduction in retraction velocity of the lamella by one order of magnitude compared to the drop of pure water. However, a dilute polymer solution has a shear viscosity and surface tension similar to that of pure solvent [11,20,21], making such a dramatic difference in behaviour surprising.

Under a strong elongational velocity gradient, polymers in a random coil experience a differential drag, resulting in a transition to a stretched out state (coil-stretch transition) [22,23]. From a macroscopic point of view, the ensemble of molecules undergoing a coil-stretch transition causes an increase of the so-called extensional (or elongational) viscosity, the ratio of the normal stress difference to the extension rate. A droplet spreading on a surface results in an elongational flow and hence it was proposed that this temporary change in the extensional viscosity dissipated sufficient energy to prevent droplet rebound.

Several problems have however been identified with this interpretation. Firstly, the velocity of the contact line during spreading is found to be the same for both the water and PEO drop. Secondly, when interfacial effects are removed by impact on small targets or heated surfaces the retraction velocity of water and PEO drops are similar [20,21,24]. However, these measurements are indirect, measuring purely the motion of the contact line and not the bulk of the drop.

We describe a novel experimental technique which enables measurements of the fluid velocity as a function of time and radial position to be performed on an impacting droplet. We subsequently apply this technique, comparing the fluid velocity inside water and viscoelastic drops (200ppm PEO water solution), allowing a better understanding of the anti-rebound effect mechanism [25].

2 Experimental setup & technique description

Our experimental setup is shown schematically in figure 1. The system is constructed around an inverted microscope (Axiovert 200, Zeiss) containing a x40 microscope objective (NA 0.75, Plan-NeoFluar, Zeiss) which was chosen for its low autofluorescence. Illumination is provided by a pulsed UV laser (365nm, mean power ∼5mw, Photonics Solutions) which produces ∼1ns pulses at a frequency of ∼8kHz. The laser is mounted on a fully adjustable translation mount. The beam was then collimated and expanded (Thorlabs) and focussed into the rear focal plane of the objective. The light entering the rear of the objective is reflected from a dichroic mirror (FT 510). This resulted in an approximately uniform illumination of the entire visible focal plane. Fluorescence from the focal plane is collected by the same objective before being filtered with a low pass spectral filter (LP 515). The field of view was recorded using a high speed CMOS camera (Phantom V9.1) equipped with a monochrome image intensifier (IL90, Lambert Instruments).

In order to visualise the flow a small quantity (∼0.001wt%) of 2μm fluorescent tracer particles (Brookhaven) were then added to the fluid. At such low concentrations the particles have no discernible effect on the droplet impact dynamics but fluoresce brightly when excited by the laser light. Since the diameter of the particles is small, their motion can be understood to faithfully reflect the underlying motion of the fluid [3]. Drops were formed using a syringe gauge at the end of a blunted hypodermic needle and detached under their own weight. The properties of the two types of drop are summarised in table 1. The hypodermic needle was carefully positioned above the objective using a micrometer adjusted mount. The mount enabled the needle to be moved radially relative to the objective, allowing the observation of different radial positions within the impacting drop. Above the objective on the microscope stage a thin glass coverslip (AGAR scientific, #0) coated with a thin film of Fluropel® was used as our hydrophobic test substrate (contact angle ∼ 106°). The plane of focus was set to a height of 10μm ± 2 above the glass substrate. The falling drops passed through an optical gate which triggered the high speed camera to collect a series of images at 2000fps.

Figure 2 (bottom) shows part of a typical image collected during the spreading of a droplet. Since the laser produces 8000 pulses per second and the camera records at 2000 fps it follows that the single particle shown moving through the field of view was exposed 4 times. Hence the central diagram in figure 2 shows 3 particles each exposed 4 times. Knowing the time between laser pulses, these particle streaks enable us to measure the velocity of the fluid by measuring the distance travelled by each particle ($V_{fluid} = \triangle x_{colloid}/\triangle t_{laser}$). Since the measurements depend quite critically upon the frequency of the laser, the time between pulses was verified in the following way. A small puddle of concentrated fluorescent colloidal solution was placed on a clean coverslip. The high speed camera was then set to record at a frame rate of 100,000 fps. The number of pulses of light captured in 1500 frames was then used

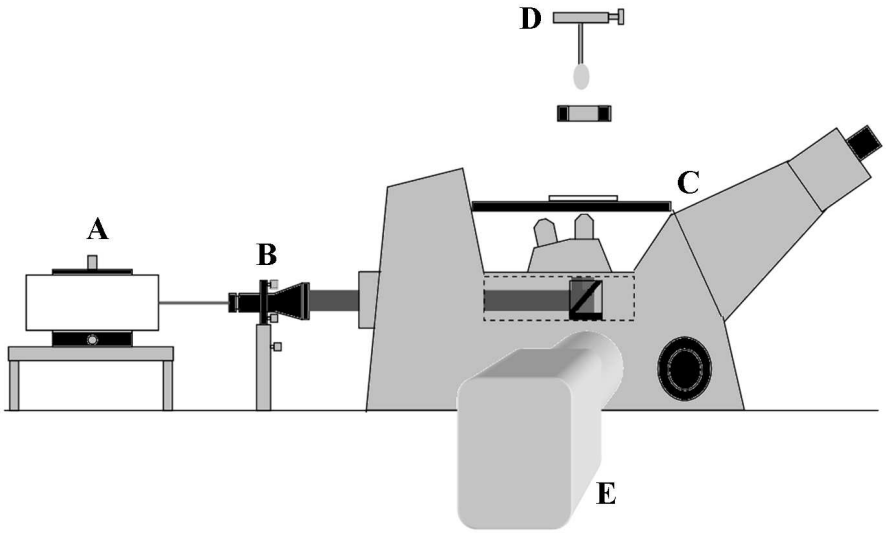

Fig. 1 Schematic of the experimental set up. A) A pulsed UV laser is used to excite 2μm fluorescent colloids inside an impacting water droplet. B) The beam is collimated and expanded by an adjustable beam expander. C) The beam is reflected from a dichroic mirror and focussed through a x40 microscope objective. The collected image is filtered using a low pass filter. D) The drop is created at the end of a blunt needle. As it falls the drop passes through a light gate which E) triggers a high speed camera, fitted with image intensifier, to record a movie at 2000fps.

to determine the laser frequency. The spatial resolution of the microscope was also measured using a calibration standard. The precise impact position of each droplet was found to vary between drops, due to the inherent instability of detachment. However, it was noted that with the exception of the very edge of the spreading droplet, particles followed radial paths during spreading. By calculating the intersection of linear fits to the particle streaks it was possible to determine the centre of the drop impact and hence the radial coordinate for particles within each frame (See figure 2). Time coordinates were measured relative to the triggering of the camera by the falling drop. By collecting series of images at different radial positions it was possible to map out the fluid velocity as a function of both time and radius (Figures 3, 4, 6).

3 A comparison of water & 200ppm PEO solution

Using this technique we compared the fluid velocities inside impacting drops of water and dilute solutions of poly-(ethylene oxide) (PEO). PEO, at a concentration of 200ppm, was slowly dissolved in deionised water which was stirred continuously with a magnetic stirrer. Table 1 summarises the properties of the two fluids used.

Drops were released from a height of 100mm resulting in an impact speed of $\sim$ 1400mms^{-1} (We$_{water}$ $\sim$ 75.1, We$_{PEO}$ $\sim$ 74.5). As the spreading drop passes over the objective, a small increase in the background intensity is observed followed by

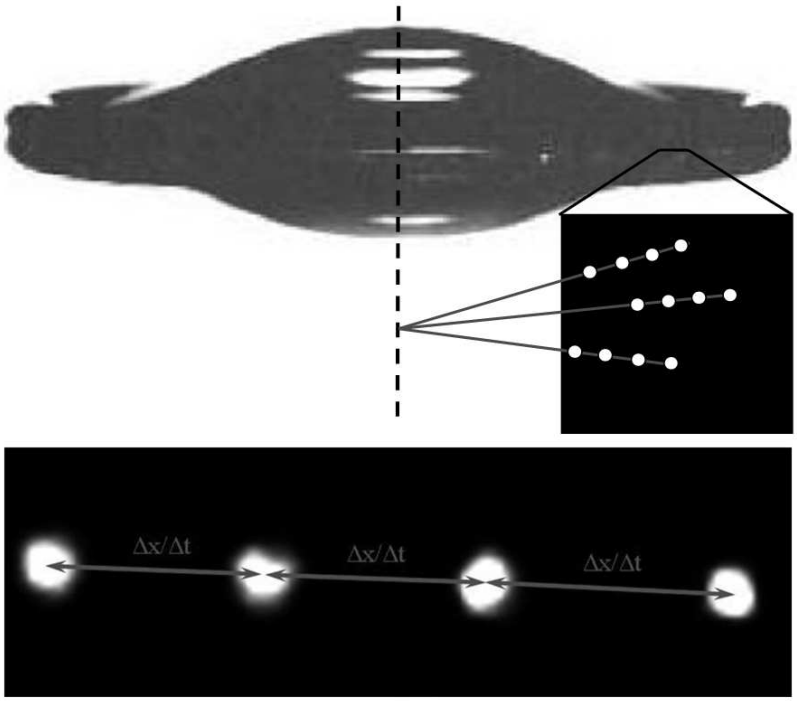

Fig. 2 PIV analysis: Top) Sideview of a spreading water drop on a hydrophobic surface. Middle) Diagram showing collection of images at a particular radial position. Colloids appear as bright fluorescent spots each exposed four times by the laser. Hence the diagram illustrates only 3 colloids. Extrapolation of the radial paths of multiple colloids can be used to find the central point of the drop and hence the radial coordinate of each measurement. Bottom) Part of a typical image of a single fluorescent colloid inside a spreading drop of water. The fluid velocity can be measured since $V_{fluid} = \triangle x_{colloid}/\triangle t_{laser}$.

Table 1 Water and PEO drop properties

Fluid	Water	200ppm PEO
Drop Diameter (mm)	2.76 ± 0.14	2.66 ± 0.1
Density at 20^{o}C (kg/m^3)	1000	1000
Viscosity at 20^{o}C (mPa.s)	1	1.23
Surface Energy at 20^{o}C (mJ/m^2)	72	70

a series of particles carried along by the fluid. For drops of pure water and those with PEO additives, particles are observed to follow radial paths during spreading. As the fluid slows a sudden reversal in the direction of the flow is observed as the drop begins to retract. Movies were collected at different radial positions up to about 80% of the maximum spreading radius. Beyond this position instabilities in the fluid cause

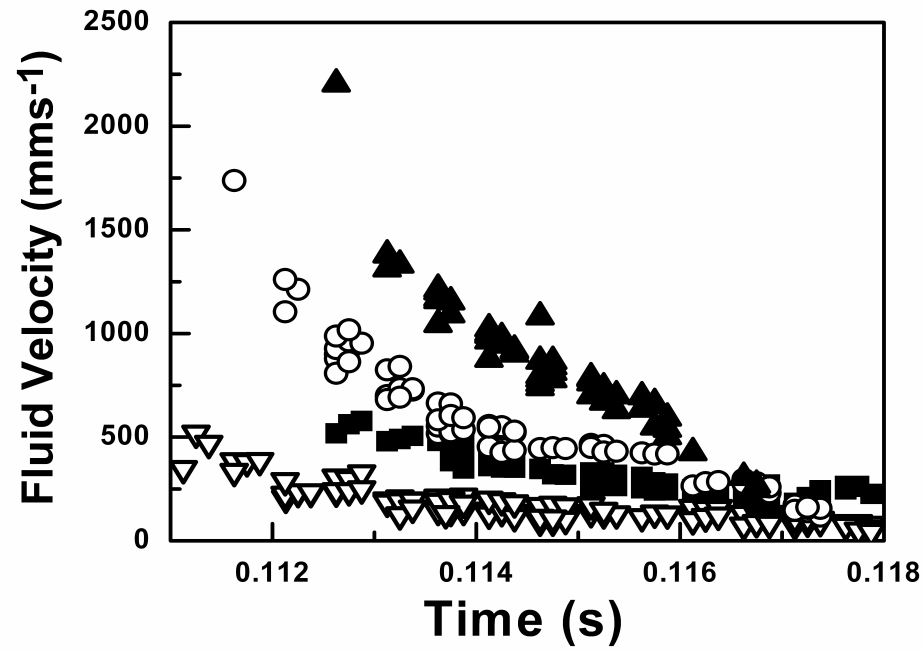

Fig. 3 Particle Image Velocimetry of Water drops impacting a hydrophobic substrate(radii ▽ 0.7, ■ 1.3, ○ 1.6, ▲ 2.8 mm). As time increases the fluid slows before retracting.

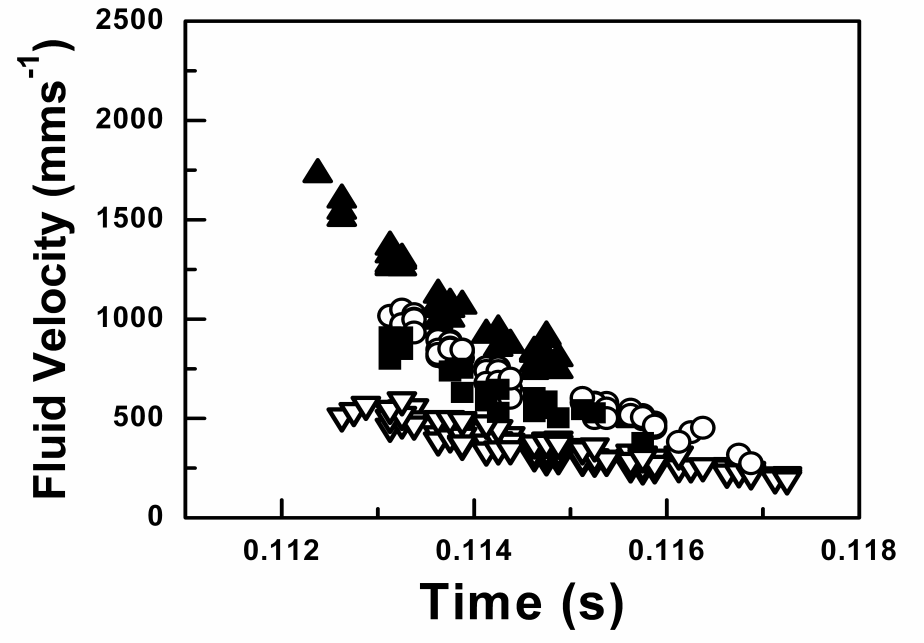

Fig. 4 Particle Image Velocimetry of 200ppm PEO drops impacting a hydrophobic substrate (bottom, radii ▽ 1.2, ■ 2.0, ○ 2.1, ▲ 2.7 mm). As time increases the fluid slows before retracting.

particles to deviate a significant amount from the usual radial paths, making location of the centre of drop impact impossible.

3.1 The spreading stage

Figures 3 & 4 show some example plots of the velocity as a function of time at different radial positions for both water and PEO drops. Upon impact the drop spreads rapidly with the velocity increasing as a function of radius and decreasing as a function of time as is expected. After approximately 0.118s the fluid velocity is observed to drop almost to zero.

Considering a momentum balance in the radial direction of the spreading droplet theory predicts the velocity field inside the lamella should obey V = r /(t + τ) [13,14], for t $\gg D_0/U_0$ (where D_0 is the initial drop diameter and U_0 is the impact velocity). Figure 5 shows the spreading of the water droplet with the radial coordinate divided by the velocity plotted against the time. A linear fit to all the data before t = 0.116s is also shown. This clearly indicates the validity of the proposed model not only for the lamella thickness as previously demonstrated [26] but also in the bulk fluid of the drop. All measurements of time were taken relative to the triggering of a light gate by the falling drop, but a good estimate of the time of impact can be made by observing the movies collected near the centre of the drop. All movies which show the centre of the drop impact indicate drop impact occurs at t=0.110 $\pm$ 0.0005s. Calculation of the intersection of the line of best fit with t = 0.110s suggests a value of $\tau \sim 0$ within the experimental error. For our system $D_0/U_0 \sim$ 0.002s therefore we expect to see little departure from a linear fit at small times. As the droplet approaches maximum spreading the velocity approaches its minimum value leading to a deviation from the linear trend.

Comparison of the fluid velocities presented in figures 3 & 4 is easier when they are plotted as a function of the radial position for both PEO and water (see figures 6 & 7). Little difference between the two fluids is apparent. This conclusion is further strengthened by comparing the velocity gradients in the fluid as a function of time (a parameter which determines whether a polymer undergoes a coil-stretch transition) which is shown in figure 8. The values observed for the dilute PEO solutions are almost identical to those of water, suggesting similar amounts of dissipation throughout the spreading of the droplet. Since the two drops have the same impact velocity, surface tension, shear viscosity and density the only parameter that could cause differences in spreading behaviour is the extensional viscosity caused by polymers stretching in the flow. However, our measurements show that at least in the bulk fluid no such differences are observed. This raises serious doubts about any significant role for extensional viscosity in suppressing droplet rebound. The magnitude of the velocity gradients measured in the fluid appears totally consistent with such an interpretation. Measurements by Crooks et al [11] of the Trouton ratio (extensional viscosity / shear viscosity) suggest that no significant increases are observed below extension rates $\sim$ 1000 s^{-1}. It therefore appears that during spreading, at the impact velocities considered, extensional viscosity is not an important parameter.

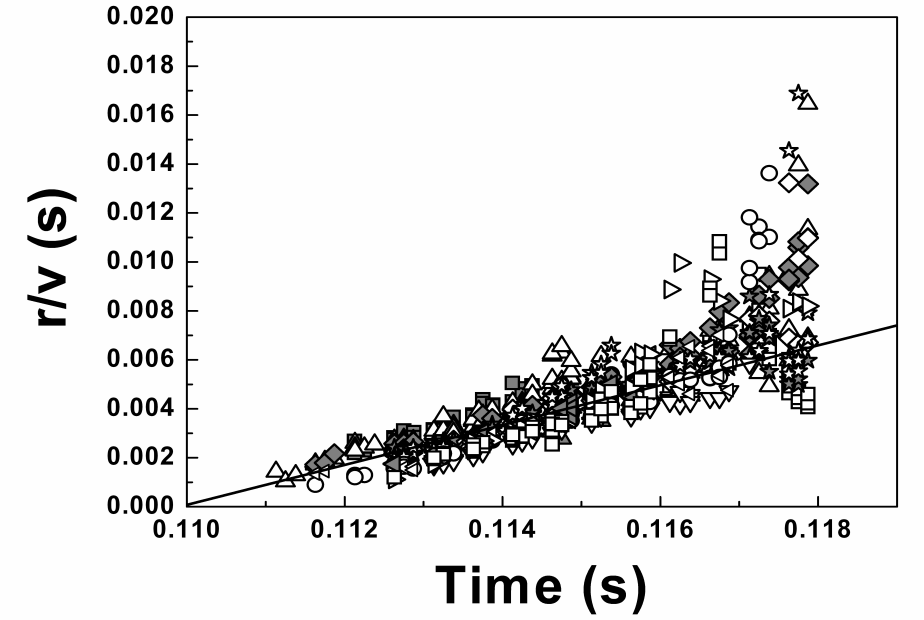

Fig. 5 Validation of the Roisman-Yarin theoretical prediction of the fluid velocity inside the spreading drops (see main text for details). The linear best fit yields r/v = 0.81t - 0.09. Drop impact occurs at t = 0.110s.

3.2 The retracting stage

The fluid gains its maximum retraction velocity on a timescale that is comparable with 1 or 2 frames of the captured sequences of images. Observation of the recorded movies appears to show that as the spreading fluid slows almost to zero, a wave of fluid from the edge of the retracting drop sweeps across the field of view leading to a jump in fluid velocity.

Velocity profiles for the retracting PEO drop show significantly smaller fluctuations in the velocity as a function of time. This is consistent with recent direct numerical simulations showing a reduction of small-scale convective motions in dilute polymer solutions [27]. Figures 9 & 10 show the retraction velocity of water and PEO drops. Despite significant scatter in the data it is clear that radial velocity gradients in both cases are small (ie $\ll 1000s^{-1}$). The fluid elements are also in compression rather than extension, making the stretching of molecules in the drop interior unlikely. A comparison of the fluid velocity in the bulk of the droplet with those values extracted from macroscopic observations of the contact line shows a dramatic difference between water and PEO drops. The motion of the contact line for droplets of pure water is similar to that of the bulk fluid. By contrast the motion of the contact line for PEO drops is ~ 1 order of magnitude slower than that of the corresponding bulk velocity measurements [25]. This difference implies that the difference between the two fluids lies solely at the droplet edge. A linear fit to the retraction velocity data reveals initial velocity gradients for water and PEO drops of 107 ± 15 and 32 ± 17 respectively. If the drop edge were responsible for the antirebound effect we would expect this to slow the

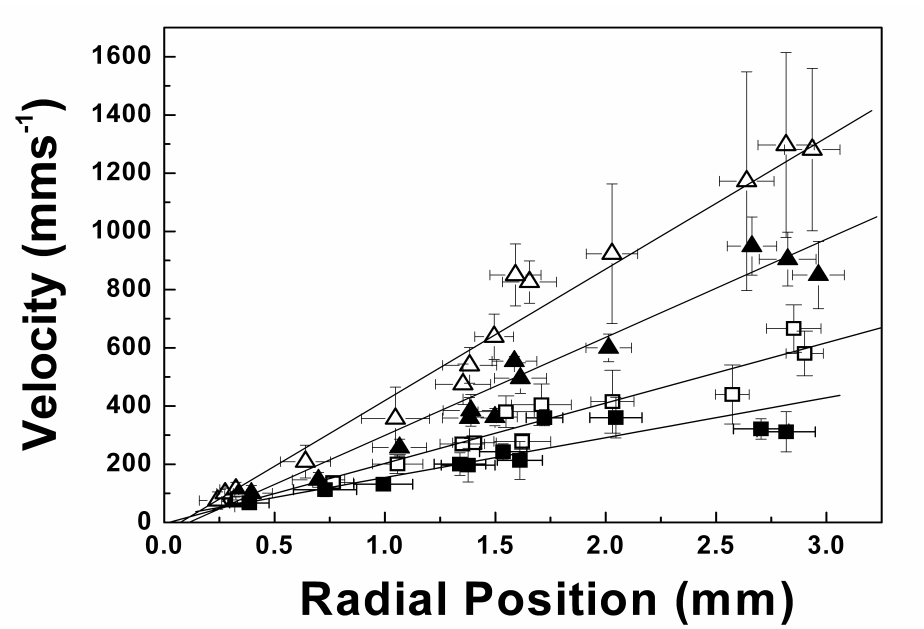

Fig. 6 Velocity profile in the spreading water drop. The measured velocities from each data set are averaged over certain time windows (△ 0.1125-0.11375, ▲ 0.11375-0.115, □ 0.115-0.11625, ■ 0.11625-0.1175). The vertical error bars reflect the standard deviations in the measured velocities. The velocity gradient inside the drop is linear at all measured times.

fluid nearest the drop edge first. This is indeed what is observed in figures 9 & 10. Data points near the centre of the drop are indistinguishable within error whilst those near the edge show a small but measurable difference. The critical role of the contact line is supported by recent measurements of the dynamic contact angle of retracting drops [25, 28] and direct visualisation of DNA, stretching at the receding drop edge [25]. The anti-rebound phenomenon therefore cannot be a result of changes in the extensional viscosity of the drop.

4 Conclusions

A novel high speed microscopy technique to enable the visualisation and quantification of flows inside an impacting drop was successfully built and demonstrated. The technique was then applied to two different problems. Firstly, our measurements of the velocity field inside the lamella were used to confirm the Roisman-Yarin model for an impacting Newtonian droplet, spreading on a surface. Secondly, by comparing the fluid velocities inside impacting drops of water and 200ppm PEO we were able to exclude the extensional viscosity as a significant factor in the anti-rebound effect during both spreading and retraction stages.

Acknowledgements The authors would like to thank Mr Bobby Hogg for technical help and Dr Ilia Roisman for insightful discussions.

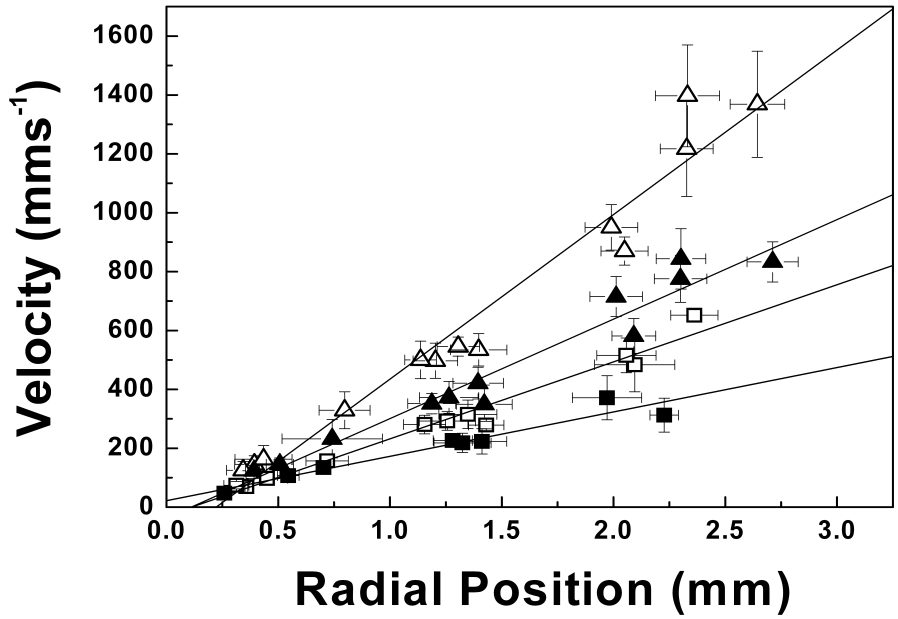

Fig. 7 Velocity profile in the spreading 200ppm PEO drop. The measured velocities from each data set are averaged over certain time windows(△ 0.1125-0.11375, ▲ 0.11375-0.115, □ 0.115-0.11625, ■ 0.11625-0.1175).

References

1. Westerweel J, (1997) Fundamentals of digital particle image velocimetry, Meas. Sci. Tech, 8(12): 1379
2. Tropea C, Yarin AL, Foss JF, (2007) Springer Handbook of Fluid Mechanics, Springer
3. Adrian RJ, (2005) Twenty years of particle image velocimetry, Expts Fluids, 39(2): 159-169
4. Bertola V, (2003) Two-Phase Flows Measurement Techniques, in: Modelling and Experimentation in Two-Phase Flow, CISM Courses and Lectures, 450, 281-323
5. Adrian RJ, (1991) Particle-imaging techniques for experimental fluid mechanics, Annu. Rev. Fluid Mech. 23:261-304
6. Yarin AL, (2006) Drop Impact Dynamics: Splashing, Spreading, Receding Bouncing..., Annu. Rev. Fluid Mech., 38:159-194
7. Rein M, (1993) Phenomena of liquid drop impact on solid and liquid surfaces, Fluid Dyn. Res., 12(2):61
8. Berberovic E,van Hinsberg NP, Jakirlic S, Roisman IV and Tropea C, (2009) Drop impact onto a liquid layer of finite thickness: Dynamics of cavity evolution Phys. Rev. E 79(3):036306
9. Williams PA, English RJ, Blanchard RL, Rose SA, Lyons L and Whitehead M, (2008) The influence of the extensional viscosity of very low concentrations of high molecular mass water-soluble polymers on atomisation and droplet impact, Pest Manag. Sci. 64(5):497
10. Bergeron V, Bonn D, Martin JY and Vovelle L, (2000) Controlling droplet deposition with polymer additives, Nature 405(6788):772
11. Crooks R, Cooper-Whitez J and Boger DV, (2001) The role of dynamic surface tension and elasticity on the dynamics of drop impact Chem. Eng. Sci. 56(19):5575
12. Roisman IV, (2009) Inertia dominated drop collisions. II. An analytical solution of the Navier-Stokes equations for a spreading viscous film, Phys. Fluids 21:052104
13. Yarin AL, Weiss DA, (1995) Impact of drops on solid surfaces: self-similar capillary waves, and splashing as a new type of kinematic discontinuity, J. Fluid Mech. 283:141-173
14. Roisman IV, Rioboo R, Tropea C, (2001) Normal impact of a liquid drop on a dry surface: model for spreading and receding, Proc. R. Soc. Lond. A 458:1411-1430

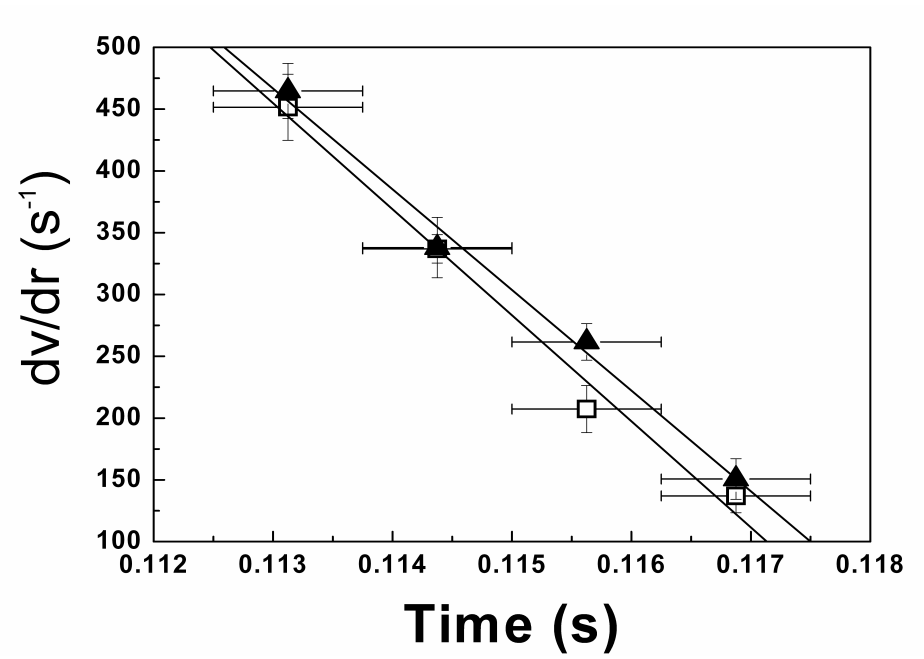

Fig. 8 A comparison of spreading in a water (□) and 200ppm PEO (▲) drop. Both drops exhibit similar velocity gradients with respect to time. Changes in extensional viscosity should be observed through changes in the velocity profile yet both fluids are clearly similar.

15. Eggers J, Fontelos MA, Josserand C and Zaleski S, (2010) Drop dynamics after impact ona solid wall:theory and simulations Phys. Fluids 22(6):062101
16. Šikalo Š, Wilhelm HD, Roisman IV, Jakirlić S, Tropea C, (2005) Dynamic contact angle of spreading droplets:experiments and simulations, Phys. Fluids 17:062103
17. Fukai J, Zhao Z, Poulikakos D, Megaridis CM, (1993) Modelling of the deformation of a liquid droplet impinging upon a flat surface, Phys. Fluids A 5:2588-2599
18. Kang KH, Lee SJ, Lee CM and Kang IS, (2004) Quantitative visualisation of flow inside an evaporating droplet using the ray tracing method, Meas. Sci. Technol. 15(4):1104-1112
19. Yarin AL, Brenn G, Kastner O, Rensink D, Tropea C, (1999) Evaporation of acoustically levitated droplets, J. Fluid Mech. 399:151-204
20. Bertola V, (2004) Drop impact on a hot surface: effect of a polymer additive, Expts Fluids 37(5):653-664
21. Bertola V, (2009) An experimental study of bouncing leidenfrost drops: Comparison between Newtonian and viscoelastic liquids, Int. J. Heat Mass Transfer 52(7):1411
22. de Gennes PG, (1974) Coil-stretch transition of dilute flexible polymers under ultrahigh velocity gradients, J. Chem. Phys. 60(12):5030
23. Keller A and Odell JA, (1985) The extensibility of macromolecules in solutions; a new focus for macromolecular science, Colloids Polym. Sci. 263(3):181-201
24. Rozkhov A, Prunet-Foch B and Vignes-Adler M, (2003) Impact of drops of polymer solutions on small targets, Phys. Fluids 15(7):2006
25. Smith MI and Bertola V, (2010) Effect of polymer additives on the wetting of impacting droplets, Phys. Rev. Lett. 104(15):154502
26. Bakshi S, Roisman IV, Tropea C, (2007) Investigations on the impact of a drop onto a small spherical target, Phys FLuids 19:032102
27. G. Boffetta, A. Mazzino, S. Musacchio and L. Vozella, Phys. Rev. Lett. 104(18):184501 (2010).
28. Bertola V, (2010) Effect of polymer additives on the apparent dynamic contact angle of impacting drops, Colloids and Surfaces A: Physicochemical and Engineering Aspects, 363(1-5):135-140

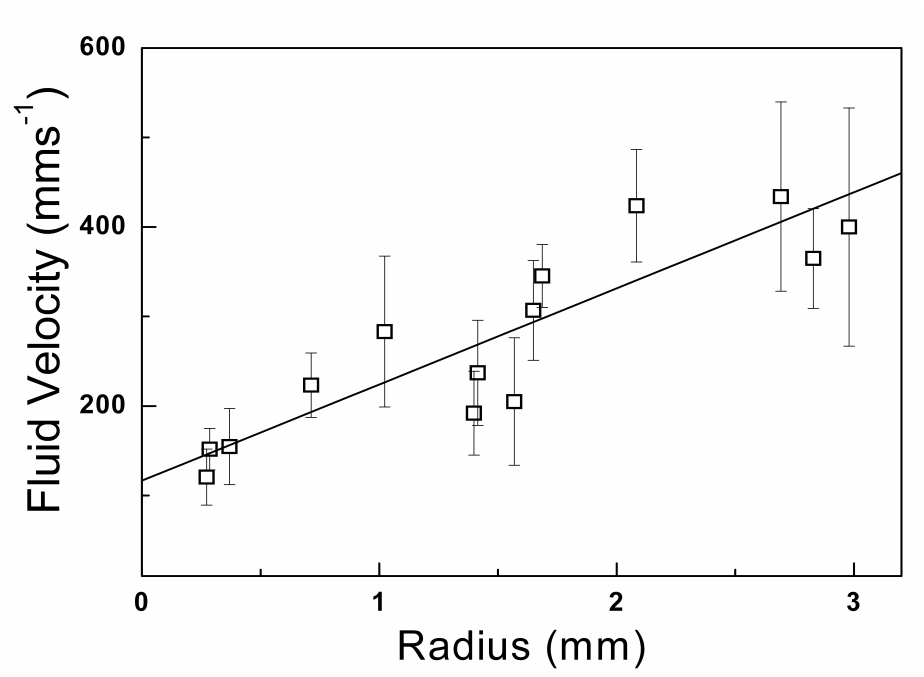

Fig. 9 Retraction velocities inside retracting drops of water. The vertical error bars represent the standard deviation of velocities observed during the initial retraction of the drop for each experiment.

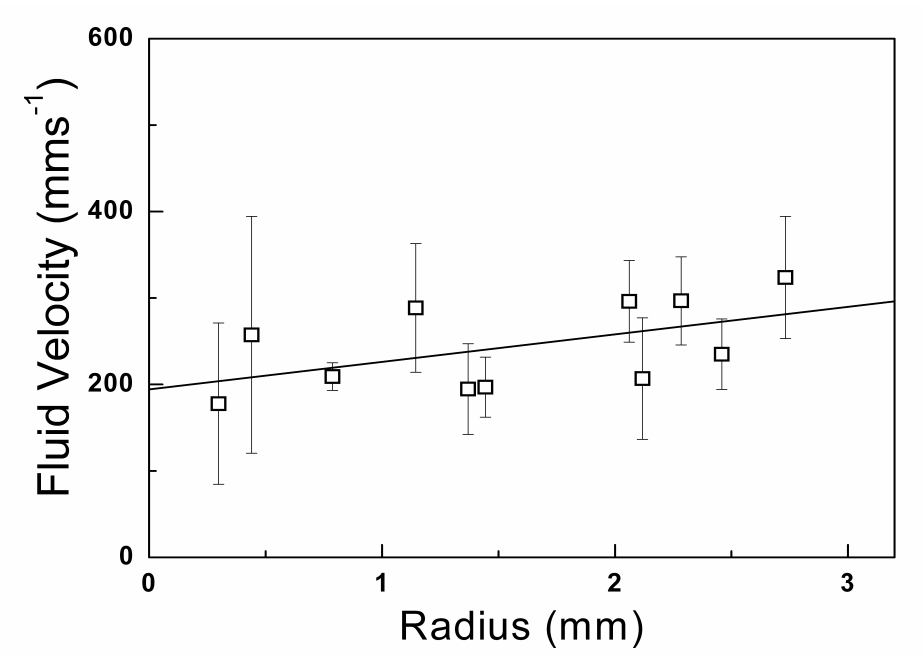

Fig. 10 Retraction velocities inside retracting drops 200ppm PEO solution. The fluid velocity inside PEO drops is similar to that of water drops, providing direct evidence that the elongational viscosity of both drops is not responsible for the anti-rebound effect (During retraction the contact line of PEO drops is known to retract an order of magnitude more slowly than for water). This suggests that the origin of the anti-rebound effect is a drop edge effect.